Supplementary Information (SI) for New Journal of Chemistry.

Supporting information

Halogen-tuned organic-inorganic hybrid perovskite semiconductor bandgap engineering

Hui-Yi Hu[#a], Ya-Xin Xu[#a], Shu-Ting Yuan[a], Jing-Yang Ma[a], Guang Xia[a], Shu-Ting Shi[a], Zi-Xiong Zhou[a], Jin-Bin Yuan*[b], Li-De Yu*[a]

a School of Pharmacy, Jiangxi University of Traditional Chinese Medicine, Nanchang 330004, Jiangxi Province, P.R. China.

b Key Lab of Modern Preparations of Traditional Chinese Medicine, Jiangxi University of Chinese Medicine, Nanchang 330004, Jiangxi Province, P.R. China.

# The authors contributed equally: Hui-Yi Hu, Ya-Xin Xu.

*Correspondence and requests for materials should be addressed to J.-B. Y. and L.-D. Y. (kings2008@163.com and 20020680@jxutcm.edu.cn).

Supplementary Index

Supplemental Experimental Procedures

Supplemental Figures

Supplemental Tables

Supplemental Experimental Procedures

Synthesis

Materials: PbI_2 (98%, Shanghai Macklin Biochemical Co., Ltd.), (*R*)-(-)-3-Quinuclidinol (98%, Nanjing Crystal Chemical Co., Ltd.), Chloroiodomethane (97%, Shanghai Titan Scientific Co., Ltd.), Dibromomethane (99%, Shanghai Titan Scientific Co., Ltd.), Diiodomethane (99%, Shanghai Titan Scientific Co., Ltd.), Hydriodic Acid (55-57 wt.%, Shanghai Titan Scientific Co., Ltd.). All chemicals are commercially available and used directly without purification.

Synthesis of compounds **1-3**: The organic amine RCM3HQ is synthesized from (*R*)-(-)-3-quinuclidinol and chloroiodomethane agitated in ethyl acetate for 6h at room temperature. The resulting product is a white solid. RBM3HQ and RIM3HQ are also prepared by the reaction of dibromomethane and diiodomethane.

The stoichiometric ratios of RCM3HQ and PbI_2 were 1:1, respectively. Using Hydriodic Acid as solvent, the hydriodic acid was slowly evaporated on a constant temperature heating table of 333 K. After about three days, a mixture containing precipitated crystal **1** and mother liquor was obtained. Similarly, crystals **2** and **3** can be obtained by using RBM3HQ and RIM3HQ as cations.

Safety statement: No uncommon hazards are noted.

General Measurements.

The Powder X-ray Diffraction (PXRD) was measured at a range of 5°–50° and a scan rate of 10°/min on the Rigaku D/MAX 2000 PC X-ray diffractometer. Differential scanning calorimetry measurements were carried out on the DSC214 Polyma instrument in the whole measured temperature range 293−453K with the rate of 15 K min^{-1} at atmospheric pressure in aluminum crucibles. For dielectric measurements, the powder samples were used as the plate with a thickness of around 0.5 mm and an area of around 6 mm^2. Carbon conducting paste deposited on the plate surfaces was used as electrodes. A Tonghui TH2828A impedance analyzer was used to measure the dielectric constants.

Single-crystal X-ray diffraction experiments.

Variable-temperature X-ray diffraction analysis was carried out using a Rigaku synergy diffractometer with Mo-Kα radiation (λ = 0.71073 Å). Data collection, cell refinement, and data reduction were performed using CrysAlisPro (version 1.171.41.112a) XtaLAB Synergy-R online system. The structures were solved by the direct method and refined by the full-matrix method based on F^2 using the OLEX2 and SHELXTL (2018) software package. All non-hydrogen atoms were refined anisotropically and the positions of all hydrogen atoms were generated geometrically. The organic cations were not modeled according to the chemical sense, because of the highly disordered form at the high-temperature phase. Detailed crystallographic data are recorded in **Tables S1–S4**. CCDC numbers: 2379968–2379970 contain supplemental crystallographic data for this article. These data are freely available from the Cambridge Crystallographic Data Centre.

X-ray detector performance measurements.

X-ray detection performance was measured on the measurement system in the DX2700B X-ray diffractometer. All X-ray response characterizations were performed directly in a dark air environment to minimize electromagnetic and ambient light interference. A DS2901/24 X-ray tube with a tungsten target and 2.4 kW output power was used as the source. Different radiation dose rates can be obtained by adjusting the values of accelerating voltage and working current. Aluminum sheets of different thicknesses were inserted between the X-ray source and the detector as attenuators. The X-ray radiation dose rate was also calibrated using an Accu-Gold digitizer.

DFT calculation

The first-principles DFT calculations were performed with the projector augmented wave pseudopotentials as implemented in Vienna *ab initio* Simulation Package (VASP). The Perdew-Burke-Ernzerhof parameterization of generalized gradient approximation (GGA) was used for the exchange-correlation functional. The plane-wave cutoff energy was 550 eV. The structural relaxation and static computation of compounds **1** and **3** were carried out using *k*-point grids of 2×1×3 and 3×3×1, respectively. The convergent criterion for the energy was set to 10^{-6} eV, and the default criterion of the Hellman-Feynman force during the structural relaxation was <0.01 eV/Å for all atoms.

Supplemental Figures

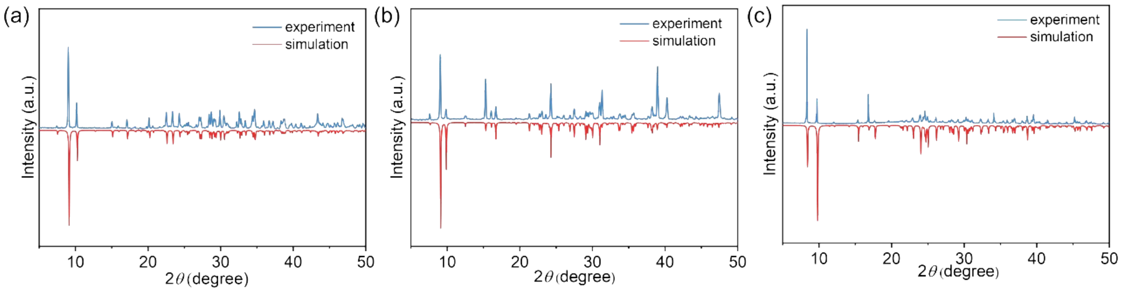

Figure S1. PXRD patterns of **1** (a), **2** (b), and, **3** (c) at 298 K.

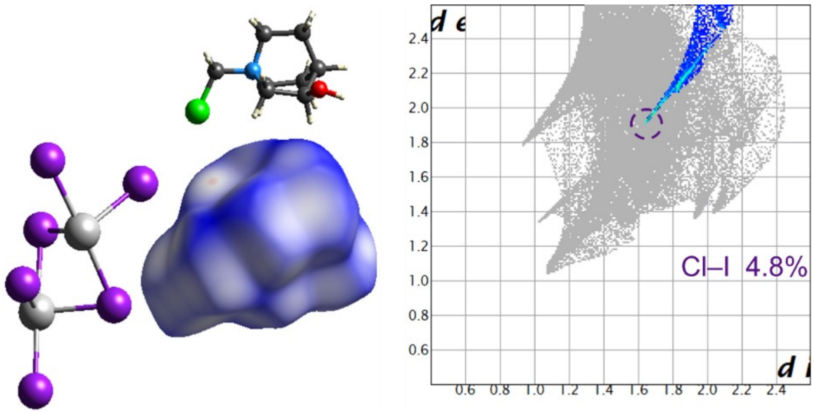

Figure S2. Hirshfeld surface analysis of hydrogen bonding interactions of the $[RCM3HQ]^+$ molecular.

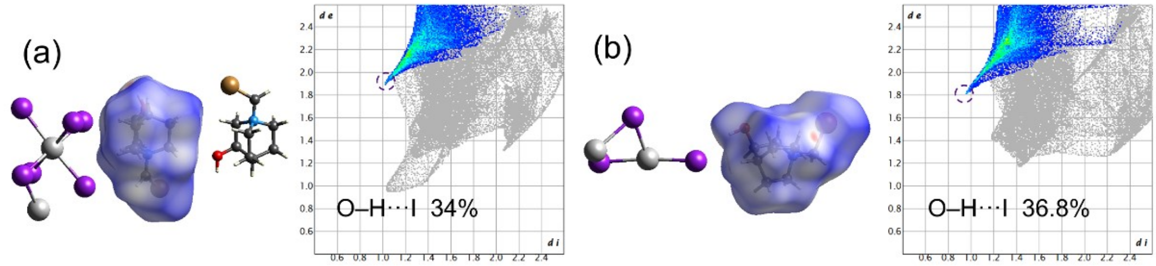

Figure S3. Hirshfeld surface analysis of hydrogen bonding interactions of the $[RBM3HQ]^+$ molecular and $[RIM3HQ]^+$.

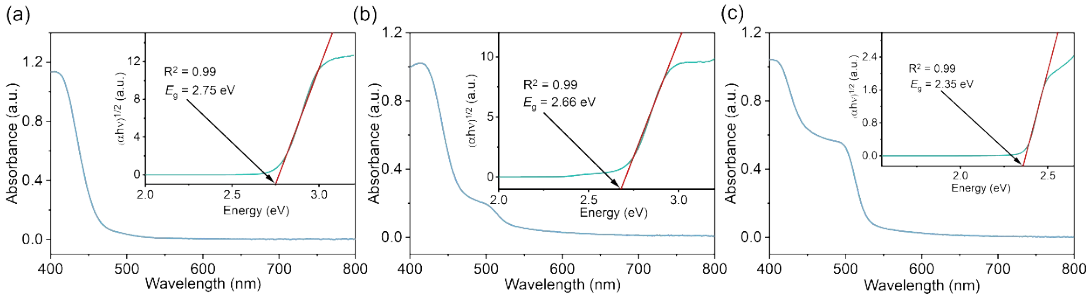

Figure S4. UV–vis absorption spectra and Tauc plots of compounds **1** (a), **2** (a), and **3** (a).

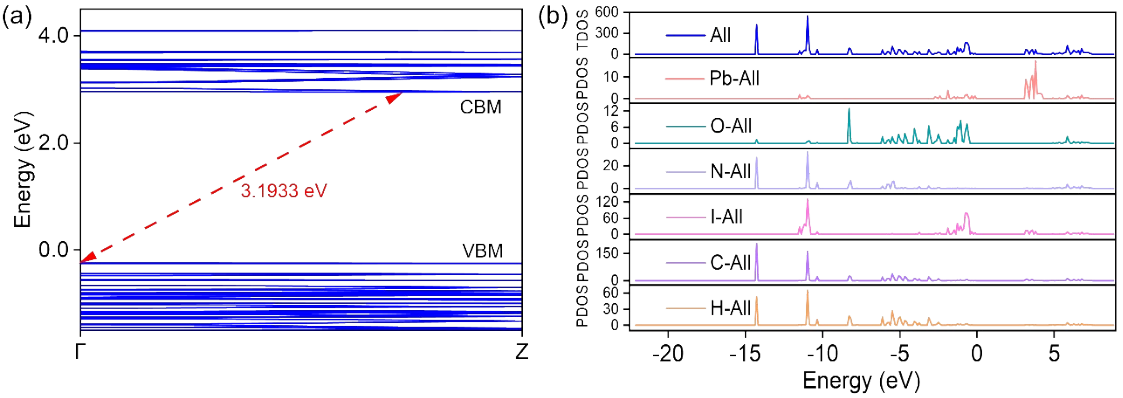

Figure S5. DFT calculations of the electronic structural features of compound **3** (a). PDOS of compound **3** (b).

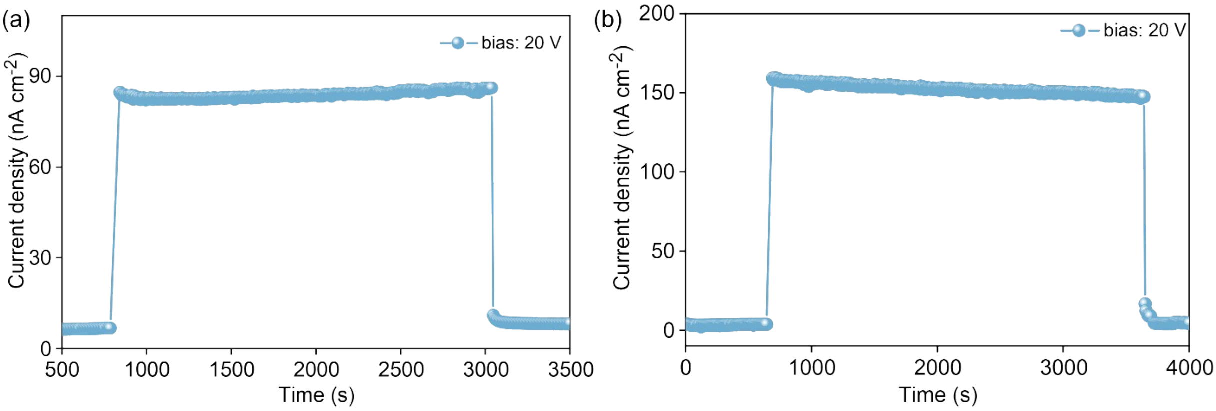

Figure S6. Stability of devices **2** (a) and **3** (b) under continuous radiation at 20 V bias.

Supplemental Tables

Table S1. Crystallographic data for compounds **1**, **2** and **3**.

Compounds	**1**	**2**	**3**
T / K	301 K	287 K	301 K
Formula	$C_{16}H_{30}Cl_2I_6N_2O_2Pb_2$	$C_{16}H_{27}Br_2I_6N_2O_2Pb_2$	$C_8H_{15}I_4NOPb$
M_w	1529.10	1614.99	856.00
Crystal system	monoclinic	orthorhombic	monoclinic
Space group	$P2_1$	$P2_12_12_1$	$I2$
a / Å	11.8334(5)	17.9058(10)	8.0496(4)
b / Å	17.2270(7)	8.0790(4)	9.9774(5)
c / Å	8.0612(3)	23.1217(11)	21.0802(13)
α / °	90	90	90
β / °	98.576(4)	90	94.908(5)
γ / °	90	90	90
V / Å^3	1624.93(11)	3344.8(3)	1686.83(16)
Z	2	4	4
D_{calc} / g·cm^{-3}	3.125	3.207	3.371
μ / mm^{-1}	16.228	17.996	17.304
F(000)	1344.0	2820.0	1488.0
2θ *range* / °	4.208−61.61	4.194−61.484	3.878−62.028
Reflns collected	15633	20563	8167
Independent reflns (R_{int})	0.0519	0.0695	0.0431
No. of parameters	274	272	137
R_1[a], wR_2[b] [I>2σ(I)]	0.0368, 0.0832	0.0712, 0.1972	0.0375, 0.0927
R_1, wR_2 [all data]	0.0532, 0.0882	0.0975, 0.2136	0.0476, 0.0966
GOF	0.954	0.983	1.010
$\Delta\rho$[c] / e·Å^{-3}	1.06/−1.28	7.54/−4.19	1.28/−1.62
CCDC	2379968	2379969	2379970

[a] $R_1 = \Sigma||F_o|-|F_c||/|F_o|$; [b] $wR_2 = [\Sigma w(F_o^2-F_c^2)^2]/\Sigma w(F_o^2)^2]^{1/2}$; [c] maximum and minimum residual electron density.

Table S2. Selected bond lengths [Å] and angles (°) for **1** at 301 K.

Pb01—I003	3.1743 (13)	I003—Pb01—I004$^{\mathrm{i}}$	84.86 (4)
Pb01—I004$^{\mathrm{i}}$	3.2940 (14)	I003—Pb01—I005	91.52 (3)
Pb01—I005	3.2169 (13)	I003—Pb01—I006$^{\mathrm{i}}$	87.05 (3)
Pb01—I006$^{\mathrm{i}}$	3.2600 (13)	I003—Pb01—I007	90.97 (3)
Pb01—I007	3.1806 (12)	I003—Pb01—I008	176.19 (4)
Pb01—I008	3.2464 (13)	I005—Pb01—I004$^{\mathrm{i}}$	176.38 (4)
Pb02—I003$^{\mathrm{ii}}$	3.2771 (13)	I005—Pb01—I006$^{\mathrm{i}}$	96.65 (3)
Pb02—I004	3.1704 (12)	I005—Pb01—I008	85.44 (3)
Pb02—I005	3.2870 (13)	I006$^{\mathrm{i}}$—Pb01—I004$^{\mathrm{i}}$	83.11 (4)
Pb02—I006	3.2110 (14)	I007—Pb01—I004$^{\mathrm{i}}$	96.27 (3)
Pb02—I007	3.2599 (14)	I007—Pb01—I005	83.84 (3)
Pb02—I008	3.1632 (13)	I007—Pb01—I006$^{\mathrm{i}}$	177.97 (4)
I003$^{\mathrm{ii}}$—Pb02—I005	96.02 (3)	I007—Pb01—I008	86.44 (3)
I004—Pb02—I003$^{\mathrm{ii}}$	85.21 (3)	I008—Pb01—I004$^{\mathrm{i}}$	98.18 (3)
I004—Pb02—I005	177.20 (4)	I008—Pb01—I006$^{\mathrm{i}}$	95.57 (3)
I004—Pb02—I006	85.89 (4)	I008—Pb02—I005	85.63 (3)
I004—Pb02—I007	95.87 (3)	I008—Pb02—I006	91.43 (3)
I006—Pb02—I003$^{\mathrm{ii}}$	86.15 (3)	I008—Pb02—I007	86.49 (3)
I006—Pb02—I005	96.69 (3)	Pb01—I003—Pb02$^{\mathrm{i}}$	77.09 (4)
I006—Pb02—I007	177.35 (4)	Pb02—I004—Pb01$^{\mathrm{ii}}$	76.89 (3)
I007—Pb02—I003$^{\mathrm{ii}}$	95.96 (3)	Pb01—I005—Pb02	76.82 (3)
I007—Pb02—I005	81.51 (3)	Pb02—I006—Pb01$^{\mathrm{ii}}$	76.83 (3)
I008—Pb02—I003$^{\mathrm{ii}}$	177.22 (4)	Pb01—I007—Pb02	77.71 (3)
I008—Pb02—I004	93.24 (3)	Pb02—I008—Pb01	78.15 (4)

Symmetry codes: (i) *x*, *y*, *z*+1; (ii) *x*, *y*, *z*−1.

Table S3. Selected bond lengths [Å] and angles (°) for **2** at 287 K.

Pb1—I5	3.2082 (18)	I5—Pb1—I3	96.20 (5)

Pb1—I3	3.2235 (18)	I5—Pb1—I4	85.25 (5)
Pb1—I4	3.2229 (17)	I5—Pb1—I1	95.12 (5)
Pb1—I1	3.2190 (17)	I5—Pb1—I2	178.16 (5)
Pb1—I2	3.2378 (18)	I5—Pb1—I6	85.87 (5)
Pb1—I6	3.2445 (19)	I3—Pb1—I2	84.75 (5)
Pb2—I5	3.1963 (18)	I3—Pb1—I6	177.16 (5)
Pb2—I3^{i}	3.1687 (18)	I4—Pb1—I3	95.24 (5)
Pb2—I4	3.2782 (18)	I4—Pb1—I2	93.10 (5)
Pb2—I1^{i}	3.2305 (18)	I4—Pb1—I6	86.86 (5)
Pb2—I2^{i}	3.2649 (19)	I1—Pb1—I3	83.65 (5)
Pb2—I6	3.3373 (19)	I1—Pb1—I4	178.86 (5)
I3^{i}—Pb2—I2^{i}	85.19 (5)	I1—Pb1—I2	86.55 (5)
I3^{i}—Pb2—I6	179.16 (6)	I1—Pb1—I6	94.24 (5)
I4—Pb2—I6	84.45 (5)	I2—Pb1—I6	93.24 (5)
I1^{i}—Pb2—I4	178.88 (6)	I5—Pb2—I4	84.53 (5)
I1^{i}—Pb2—I2^{i}	85.91 (5)	I5—Pb2—I1^{i}	94.36 (5)
I1^{i}—Pb2—I6	95.66 (5)	I5—Pb2—I2^{i}	179.65 (5)
I2^{i}—Pb2—I4	95.19 (5)	I5—Pb2—I6	84.53 (5)
I2^{i}—Pb2—I6	95.66 (5)	I3^{i}—Pb2—I5	94.63 (5)
Pb2—I5—Pb1	78.42 (4)	I3^{i}—Pb2—I4	95.53 (5)
Pb2^{ii}—I3—Pb1	78.17 (4)	I3^{i}—Pb2—I1^{i}	84.34 (5)
Pb1—I4—Pb2	77.04 (4)	Pb1—I2—Pb2^{ii}	76.60 (4)
Pb1—I1—Pb2^{ii}	77.35 (4)	Pb1—I6—Pb2	75.91 (4)

Symmetry codes: (i) x, y−1, z; (ii) x, y+1, z.

Table S4. Selected bond lengths [Å] and angles (°) for **3** at 301 K.

Pb1—I4	3.2169 (11)	I4^{i}—Pb1—I4	99.85 (4)
Pb1—I4^{i}	3.2169 (11)	I4^{i}—Pb1—I2^{i}	173.11 (4)
Pb1—I3^{i}	3.2152 (12)	I4—Pb1—I2	173.10 (4)

Pb1—I3	3.2152 (12)	I4—Pb1—I2$^{\mathrm{i}}$	86.00 (3)
Pb1—I2	3.2183 (12)	I4$^{\mathrm{i}}$—Pb1—I2	86.00 (3)
Pb1—I2$^{\mathrm{i}}$	3.2183 (12)	I3—Pb1—I4	84.94 (3)
Pb2—I4	3.2171 (12)	I3$^{\mathrm{i}}$—Pb1—I4	90.41 (3)
Pb2—I4$^{\mathrm{ii}}$	3.2171 (12)	I3—Pb1—I4$^{\mathrm{i}}$	90.41 (3)
Pb2—I3	3.2292 (11)	I3$^{\mathrm{i}}$—Pb1—I4$^{\mathrm{i}}$	84.94 (3)
Pb2—I3$^{\mathrm{ii}}$	3.2292 (11)	I3$^{\mathrm{i}}$—Pb1—I3	172.78 (5)
Pb2—I2$^{\mathrm{iii}}$	3.2917 (13)	I3$^{\mathrm{i}}$—Pb1—I2$^{\mathrm{i}}$	98.77 (3)
Pb2—I2$^{\mathrm{i}}$	3.2917 (13)	I3—Pb1—I2	98.77 (3)
I1—C1	2.123 (17)	I3$^{\mathrm{i}}$—Pb1—I2	86.44 (3)
N1—C4	1.510 (18)	I3—Pb1—I2$^{\mathrm{i}}$	86.44 (3)
N1—C3	1.48 (2)	I2$^{\mathrm{i}}$—Pb1—I2	88.42 (5)
N1—C2	1.515 (19)	I4—Pb2—I4$^{\mathrm{ii}}$	99.51 (5)
N1—C1	1.487 (19)	I4—Pb2—I3	84.71 (3)
O1—H1	0.8200	I4$^{\mathrm{ii}}$—Pb2—I3$^{\mathrm{ii}}$	84.71 (3)
O1—C5	1.396 (16)	I4$^{\mathrm{ii}}$—Pb2—I3	90.47 (3)
C4—H4A	0.9700	I4—Pb2—I3$^{\mathrm{ii}}$	90.47 (3)
I3$^{\mathrm{ii}}$—Pb2—I2$^{\mathrm{i}}$	100.25 (3)	I4—Pb2—I2$^{\mathrm{i}}$	84.78 (3)
I3$^{\mathrm{ii}}$—Pb2—I2$^{\mathrm{iii}}$	85.00 (3)	I4$^{\mathrm{ii}}$—Pb2—I2$^{\mathrm{i}}$	173.47 (3)
I2$^{\mathrm{i}}$—Pb2—I2$^{\mathrm{iii}}$	91.38 (5)	I4$^{\mathrm{ii}}$—Pb2—I2$^{\mathrm{iii}}$	84.79 (3)
Pb1—I4—Pb2	77.45 (3)	I4—Pb2—I2$^{\mathrm{iii}}$	173.47 (3)
Pb1—I3—Pb2	77.30 (3)	I3$^{\mathrm{ii}}$—Pb2—I3	172.55 (5)
Pb1—I2—Pb2$^{\mathrm{iv}}$	76.37 (3)	I3—Pb2—I2$^{\mathrm{iii}}$	100.25 (3)
I3—Pb2—I2$^{\mathrm{i}}$	85.00 (3)		

Symmetry codes: (i) $-x+2, y, -z+1$; (ii) $-x+3, y, -z+1$; (iii) $x+1, y, z$; (iv) $x-1, y, z$.

Table S5. Bond lengths [Å] and bond angles [°] of the hydrogen bond of **1, 2** and **3**.

1

D−H···*A*	*D*−H	H···*A*	*D*···*A*	*D*−H···*A*

C00D−H00*B*···Cl09	0.97	2.73	3.146 (10)	106
C00F−H00*K*···Cl0*A*	0.97	2.70	3.144 (11)	109
C00H−H00*F*···Cl09	0.97	2.70	3.053 (9)	102
C00H−H00*F*···O16$^{\text{i}}$	0.97	2.46	3.337 (17)	150
C19−H19*A*···O18$^{\text{iii}}$	0.97	2.84	3.24 (2)	106
C19−H19*B*···Cl0*A*	0.97	2.75	3.103 (9)	102
C1−H1*B*···O16	0.97	2.78	3.096 (19)	100

Symmetry codes: (i) x, y, z+1; (iii) −x+2, y−1/2, −z+1.

2

D−H···*A*	*D*−H	H···*A*	*D*···*A*	*D*−H···*A*
C6−H6*A*···Br2	0.97	2.87	3.271 (15)	106
C6−H6*B*···O2	0.97	2.74	3.19 (3)	109
C5−H5*B*···Br2	0.97	2.88	3.265 (14)	104
C15−H15*B*···Br1	0.97	2.76	3.155 (14)	105
C14−H14*A*···Br1	0.97	2.91	3.313 (15)	106
C14−H14*B*···O1$^{\text{iii}}$	0.97	2.45	3.35 (3)	155

Symmetry code: (iii) *x*+1/2, −*y*+3/2, −*z*+1.

3

D−H···*A*	*D*−H	H···*A*	*D*···*A*	*D*−H···*A*
C3−H3*A*···O1$^{\text{v}}$	0.97	2.65	3.11 (2)	110
C7−H7*A*···O1	0.97	2.63	2.964 (16)	100

Symmetry code: (v) −*x*+1/2, *y*−1/2, −*z*+1/2.

Table S6. The volume fraction of organic cation of compounds **1**, **2** and **3** in the low temperature phase.

Compounds	X(av)	Y(av)	Z(av)	Total potential solvent area vol	Per unit cell vol	ratio

1	-0.013	0.275	-0.039	1029.7	1624	63.4 %
2	-0.005	-0.041	0.002	2152.4	3344.8	64.4 %
3	0.004	-0.064	0.194	1089.1	1686..8	64.6 %